A Sparse Unified Structural Equation Modeling Approach for Brain Connectivity Analysis

Xiaohui Chen, Z. Jane Wang
Department of Electrical & Computer Engineering,
University of British Columbia,
Vancouver, BC, V6T 1Z4, Canada
Email: xiaohuic,zjanew@ece.ubc.ca

Martin J. McKeown
Pacific Parkinson's Research Center
Department of Medicine (Neurology)
University of British Columbia,
Vancouver, BC, V6T 2B5, Canada
Email: mmckeown@interchange.ubc.ca

***Abstract*—Recent work has emphasized the importance of functional connectivity in normal brain functioning, especially when it can be inferred non-invasively using technologies such as fMRI. Ideally, models applied to fMRI data, such as structural equation modeling (SEM) and multivariate autoregressive (mAR) modeling, should allow the discovery of effective connectivity between brain regions. Unfortunately, the performance of these models is limited in practice due to the relatively short number of time points available, as well as the large number of potentially interesting Regions of Interest (ROIs). However, based on anatomical and functional considerations, ROIs can be considered sparsely connected. We therefore propose incorporating sparsity into the so-called "unified" joint SEM and mAR approach. To solve the proposed sparse problem, we develop a new hierarchical Bayesian framework with a reversible jump Markov chain Monte Carlo (RJ-MCMC) estimation algorithm. Simulation results show the high detection efficiency of connections of the proposed framework. Application to real fMRI study in Parkinson's Disease reveals promising results. We suggest that the proposed sparse approach is more appropriate for fMRI studies, especially for the case of large networks.**

I. Introduction

With the availability of non-invasive functional neuroimaging techniques such as fMRI, there has been increasing interest in neuroscience in inferring functional connectivity and interactions between brain regions to understand brain function. Several mathematical formalisms, such as structural equation modeling (SEM) [1], multivariate autoregressive models (mAR) [2] and dynamic causal modeling (DCM), have all been suggested as ways to model effective connectivity from neuroimaging data. SEM has been the most widely used model for brain connectivity analysis [1], [3]. However, there is a major drawback to SEM pertinent to fMRI analysis: though fMRI data are multivariate times series, SEMs do not take into consideration of temporal information in fMRI. Despite the fact that the sampling period of fMRI is long (e.g. 1-2s), there still may be dependencies between ROIs at adjacent time points. To overcome this drawback, mAR models have been proposed for the analysis of fMRI data [2] to characterize the dependencies between time points and between brain regions by a matrix of weighting coefficients. Very recently, a "unified" SEM approach, which combines both SEM and mAR models, has been proposed [4] that includes longitudinal temporal relations (represented by mAR model) as well as contemporaneous relations (represented by SEM) to reflect relationships between brain regions at the same time point.

However, there is the "curse of complexity" with the above SEM and/or mAR approaches when dealing with fMRI data in practice, especially when the number of brain regions-of-interest (ROIs) is relatively large and the number of time points is limited. For instance, considering a network consisting of 20 ROIs, each increment in the MAR model order will result in an additional 400 parameters to be determined, and the usual time-series methods break down when only limited observations are available as is the case of fMRI. In addition, the underlying implicit full connection assumption in a regular SEM and/or mAR model is questionable in brain connectivity analysis, as based on anatomical and functional considerations, the connections between brain regions may be considered *a priori* to form a sparse network.

The above observations motivated us to incorporate sparsity into brain connectivity modeling. Restricting their attention to networks with sparse connectivity, Sosa et al. proposed modeling fMRI data using sparse mAR models in which the parameters are estimated using penalized regression [5]. They also examined several other penalty functions such as the ridge, lasso and SCAD [5]. In this paper, we propose incorporating sparsity into the "unified" joint SEM and mAR approach.

The contribution of this paper is two-fold: first, the sparsity or conditional independence in the brain connectivity network represented by the "unified" joint SEM and mAR model need not be specified *a priori* but is determined by the data automatically. Second, we present a new hierarchical, fully Bayesian methodology to model sparse linear regression, and propose a reversible jump Markov chain Monte Carlo (RJ-MCMC) algorithm to simulate the posterior distribution. A real fMRI study including subjects with Parkinson's Disease (PD) will be discussed to demonstrate the applicability of the proposed approach.

II. Method

A. Joint Sparse SEM and mAR Model

We propose a unified approach that combines SEM and mAR models to simultaneously capture the spatial and temporal activities of the brain. Let $\boldsymbol{y}(t) = (y_1(t), \cdots, y_p(t))^T$

be a $p \times 1$ dimensional vector, which contains the intensity measurement for the p brain ROIs at time t, for $t = 1, \cdots, T$. For mAR component of the unified model, we consider only up to an m^{th} order process. Hence, by combining the SEM part, the proposed model can be expressed as:

$$\boldsymbol{y}(t) = \underbrace{\boldsymbol{A}\boldsymbol{y}(t)}_{\text{SEM}} + \underbrace{\sum_{j=1}^{m} \boldsymbol{\Phi}(j)\boldsymbol{y}(t-j)}_{\text{mAR}} + \underbrace{\boldsymbol{\epsilon}(t)}_{\text{noise}} \tag{1}$$

where $\boldsymbol{A}$ and $\boldsymbol{\Phi}(j)$ are $p \times p$ coefficient matrices to be estimated, for $j = 1, \cdots, m$; $\boldsymbol{\epsilon}(t)$ is a noise vector which is assumed to Gaussian with zero mean and constant variance σ^2. The $\boldsymbol{A}$ matrix represents the spatial connection strengths between ROIs, while the $\boldsymbol{\Phi}(j)'$s are the time lag effect strengths. A similar unified model was first considered by Kim et.al. [4]. However, their model structure was fixed and parameters were estimated conditioned on the fixed structure. In this paper, we shall consider a flexible modeling framework, which allows the model size to be varied and prior probability is assigned to each model. Moreover, since brain connections between ROIs are usually considered to be spare, we also put a sparsity constraint on the estimated coefficients [5].

B. A Fully Bayesian Approach for Estimation

To tackle the sparse network problem in Eq.(1), we propose a powerful, fully Bayesian framework to simultaneously perform model averaging and parameter estimation. Since the posterior distribution is in a highly-complicated non-standard form, the analytic solutions for the posterior expectations of the interested parameters ($\boldsymbol{A}$ and $\boldsymbol{\Phi}(j)$) do not exist. We therefore propose a reversible jump Markov chain Monte Carlo (RJ-MCMC) algorithm to do the numeric integration. Due to space limitations, here we briefly describe the proposed model and the estimation algorithm. The details can be found in the journal version of our sparse linear regression approach in [6].

First of all, to achieve the parsimonious estimation purpose, we assign sparsity promoting priors on the coefficients. The most commonly used sparsity prior is the double-exponential (DE) prior (i.e., Laplacian prior). This prior is also equivalent to the L_1 penalized maximum likelihood estimation, which is called 'Least Absolute Shrinkage and Selection Operator' (the *lasso*) in the literature [7]. For example, here we put independent DE priors on the elements of $\boldsymbol{A}$ matrix

$$\pi(a_{ij}|\tau) = \frac{1}{2\tau} \exp\left(-\frac{|a_{ij}|}{\tau}\right) \tag{2}$$

where τ is a shrinkage tuning parameter for a_{ij}. Since we may not have prior knowledge of how much shrinkage amount should be put on the coefficients before performing any experiment, it is reasonable to assign a non-informative prior on the hyper-parameter τ. The same rationale for giving a non-informative prior for the noise variance σ^2. Together, Jeffrey's non-informative priors are put on the top level:

$$\pi(\tau, \sigma^2) \propto \frac{1}{\tau\sigma}. \tag{3}$$

On the other hand, prior probabilities are also assigned to each possible sub-models. Specifically, a model containing k predictors/elements has a right-truncated Poisson distribution. That is

$$p(k) \propto \frac{e^{-\lambda}\lambda^k}{k!} \tag{4}$$

for $k = 1, \cdots, (m+1) \times p$. Finally, to complete our fully Bayesian framework, λ has also a non-informative prior

$$\pi(\lambda) \propto \frac{1}{\lambda} \tag{5}$$

Therefore, the posterior distribution of parameters is given by (up to a multiplicative constant)

$$\begin{aligned}
&\pi(\boldsymbol{a}_i, \boldsymbol{\Phi}(1)_i, \cdots, \boldsymbol{\Phi}(m)_i, \tau, \sigma^2, k, \lambda | \boldsymbol{y}(1), \cdots, \boldsymbol{y}(T)) \\
&\propto \frac{e^{-\lambda}\lambda^{k-1}}{\binom{p}{k} k!} \tau^{-(k+1)} \sigma^{-(T-m+1)} \\
&\times \exp\left(-\frac{||\boldsymbol{a}_i^T||_1 + \sum_{j=1}^{m} ||\boldsymbol{\Phi}(j)_i^T||_1}{\tau}\right) \\
&\times \prod_{t=m+1}^{T} \exp\left(-\frac{(y_i(t) - \boldsymbol{a}_i^T \boldsymbol{y}(t) - \sum_{j=1}^{m} \boldsymbol{\Phi}(j)_i^T \boldsymbol{y}(t-j))^2}{2\sigma^2}\right)
\end{aligned}$$

where $\boldsymbol{a}_i$ and $\boldsymbol{\Phi}(j)_i$ are the i^{th} row vectors of $\boldsymbol{A}$ and $\boldsymbol{\Phi}(j)$, respectively. Here, $||\boldsymbol{a}_i||_1 = \sum_{j=1}^{p} |a_{ij}|$, the L_1 Euclidean norm of a vector.

Since this posterior distribution is highly non-standard, containing both discrete and continuous parameters, a closed-form solution for the minimum variance estimators $\mathbb{E}(\boldsymbol{A}|\boldsymbol{y}(1), \cdots, \boldsymbol{y}(T))$ and $\mathbb{E}(\boldsymbol{\Phi}(j)|\boldsymbol{y}(1), \cdots, \boldsymbol{y}(T))$ is practically impossible to compute. We must therefore use simulation-based methods to numerically compute these expectations. This problem is compatible with the RJ-MCMC umbrella, proposed by Green [8]. We therefore develop a RJ-MCMC algorithm, which allows the simulated Markov chain to jump between sub-models. Briefly speaking, the Gibbs sampler is used for the parameters τ, σ^2, λ. For the coefficients and the number of predictors in the sub-model, we adopt a *split-and-merge* strategy [9] to travel between models. Detailed modeling and algorithmic issues are available in [6].

III. SIMULATION

A simulation is used to demonstrate the advantage of the proposed fully Bayesian approach over optimization-based methods for sparse linear regression. We compare our algorithm with the lasso and Least Angle Regression (LAR) algorithms, which are implemented in the `lars` **R** package [10]. We simulate two setups with varying data dimensions $p = 45$ and 90, each of which has a sparse coefficient structure. For instance, for a 90 dimensional model, we set the coefficients to be

$$(\underbrace{3, \cdots, 3}_{\text{10 times}}, \underbrace{0, \cdots, 0}_{\text{20 times}}, \underbrace{1.5, \cdots, 1.5}_{\text{10 times}}, \underbrace{0, \cdots, 0}_{\text{20 times}}, \underbrace{2, \cdots, 2}_{\text{10 times}}, \underbrace{0, \cdots, 0}_{\text{20 times}}).$$

The number of data points n is set on a linear grid from 100 to 400, with an interval size of 50. Our RJ-MCMC is

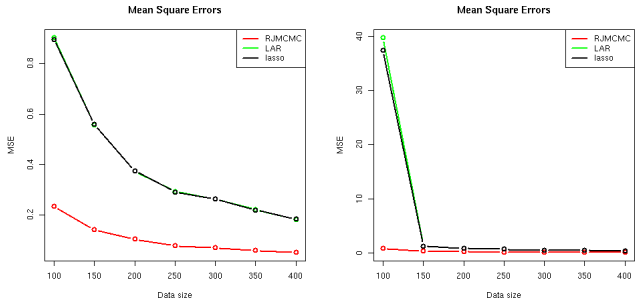

(a) $p = 45$ (b) $p = 90$

Fig. 1. MSE for the lasso, LAR, and our RJ-MCMC algorithms

TABLE I
MSEs AVERAGED OVER 100 SIMULATIONS FOR $n = 100$. THE NUMBER IN THE BRACKET IS THE STANDARD DEVIATION OF ESTIMATED MSEs.

	(True # Predictors)/(All # Predictors)	
	15/45	30/90
RJMCMC	0.233 (0.0673)	0.828 (0.193)
LAR	0.902 (0.269)	39.683 (22.951)
lasso	0.896 (0.221)	37.414 (22.980)

initialized with the Least Squares (LS) estimate for the full model and run for 100,000 iterations with the first half of the runs discarded as burn-in. Performance is measured by Mean Squared Error (MSE) and all simulation results are averaged over 100 simulations.

First, we plot the MSE against the number of data points. The results are shown in Fig.1. In general, the estimation errors measured by MSE for the proposed RJ-MCMC method is uniformly smaller than those for the lasso and LAR. In most cases, the MSEs from the lasso and LAR are more than twice as that from the proposed algorithm, and the gain from the current approach is much more significant when $p = 90$ and $n = 100$, the nearly singular case. Table I shows the MSEs for $n = 100$ case in the 2 scenarios. This simulation study therefore shows that the proposed method has much lower estimation errors than those from state-of-the-art optimization based methods.

IV. A REAL FMRI STUDY IN PARKINSON'S DISEASE

A. Data Description

Ten normal people and ten Parkinson's Disease (PD) patients participated in the study. Subjects continually squeezed a bulb in their right hand to control an inflatable ring so that the ring moved through an undulating tunnel without touching the sides. A trial of the task was five minutes. Normal subjects performed only one trial; the PD subjects performed the same task twice, once before L-dopa medication, the other after the medication.

fMRI data were collected with a Philips Achieva 3.0 T scanner with a TR interval of 2s. After motion correction, the fMRI time courses of the voxels within each ROI were averaged to represent the summary activity of each ROI. The averaged time courses were then linearly detrended and normalized to unit variance. The following eighteen brain regions were selected as the ROIs : the left and right (denoted as prefixes L or R in the abbreviated name ROIs) primary motor cortex (L M1 and R M1), supplementary motor cortex (L SMA and R SMA), lateral cerebellar hemisphere (L CER and R CER), putamen (L PUT and R PUT), caudate (L CAU and R CAU), thalamus (L THA and R THA), anterior cingulate cortex (L ACC and R ACC), globus pallidus (L GLP and R GLP), and prefrontal cortex (L PFC and R PFC).

B. Results

We use the proposed sparse linear model (c.f. Eq.(1)) on the above described 18-ROIs fMRI data set. Empirical studies showed that setting the maximum length of lag to 1 is enough for most analysis purposes [11]. By applying the proposed method, we obtain an array of estimated coefficient matrices for $\boldsymbol{A}$ and $\boldsymbol{\Phi}(1)$. For comparison, we also reported the results from the regular joint SEM and mAR model (the full model). It is noted that the regular model always yields much more connections than that of the sparse model. Though the ground truth is unknown in this real fMRI study, based on a couple of observations, we suspect that many of the connections from the regular model may be false ones. First, our simulations show that the sparse model tends to have a much lower false alarm rate, in terms of estimation error. Secondly, we note that the proposed sparse approach reveals greater consistency between models derived from subsets of the fMRI data compared to the traditional full model.

We first examined the connections that are statistically significant different across groups. We have three groups including N (normal controls), P_{pre} (PD subjects before taking L-dopa medication), and P_{post} (PD subjects on medicine on medicine). Based on the ANOVA test of estimated connections using the Bayesian sparse model, we first identify all influential connections whose values are significantly different in at least one of the three groups. Table II shows the significant connections after setting a p-value cutoff of 0.05. The regular (full) joint SEM and mAR model identifies much more significant connections. However, due to space limitation, they are not shown here. To investigate the effect of medication on the specific connections between ROIs, we simply compared the sign of the mean difference between normal and P_{pre} groups with the sign of the mean difference between patients on and off medication, where the same sign implies an effective treatment of the medication. Table II indicates that L-dopa medication has a normalizing effect on 10 connections among all 15 identified connections.

Secondly, we are interested in detecting which brain connections are affected by the disease and by the drug. To do so, we find the significant different connections between N and P_{pre}, and P_{pre} and P_{post}. The p-value cutoff is also set to 0.05. The learned network connections from our sparse model are shown in Fig.2 and Fig.4. We also show the significant

TABLE II
GROUP ANALYSIS OF SQUEEZE TASK FMRI DATA FOR OUR SPARSE METHOD. THE CONNECTION STRENGTHS ARE AVERAGED BASED ON ESTIMATED COEFFICIENTS WITHIN EACH GROUP.

Connection	N	P_{pre}	P_{post}
$R\_PUT \rightarrow L\_ACC$ (lag 0)	0.002	0	0.094
$R\_ACC \rightarrow L\_CAU$ (lag 0)	0.004	-0.011	0.093
$R\_CAU \rightarrow L\_CAU$ (lag 0)	0.487	0.429	0.269
$R\_CAU \rightarrow L\_PFC$ (lag 0)	0.006	0.001	0.039
$R\_PFC \rightarrow L\_PFC$ (lag 1)	-0.116	-0.270	-0.328
$L\_THA \rightarrow L\_PUT$ (lag 0)	0.013	0.003	0.038
$R\_M1 \rightarrow L\_PUT$ (lag 0)	-0.019	0.066	0.014
$L\_THA \rightarrow L\_SMA$ (lag 0)	0.013	0.016	0.118
$R\_SMA \rightarrow L\_SMA$ (lag 0)	0.568	0.411	0.335
$L\_ACC \rightarrow R\_GLP$ (lag 0)	-0.041	0.071	0.004
$R\_ACC \rightarrow R\_M1$ (lag 1)	0	-0.006	-0.003
$R\_CAU \rightarrow R\_M1$ (lag 1)	0	-0.013	0.0016
$R\_ACC \rightarrow R\_PFC$ (lag 0)	0.254	0.040	0.226
$R\_THA \rightarrow R\_PFC$ (lag 0)	0.021	-0.028	0.008
$L\_PFC \rightarrow R\_PFC$ (lag 1)	-0.104	-0.271	-0.349

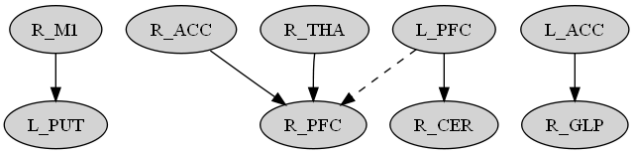

Fig. 2. The significant different connections between N and P_{pre} groups, derived from the proposed sparse model. Solid lines are the SEM connection and dashed lines are the 1[th]-order mAR connections.

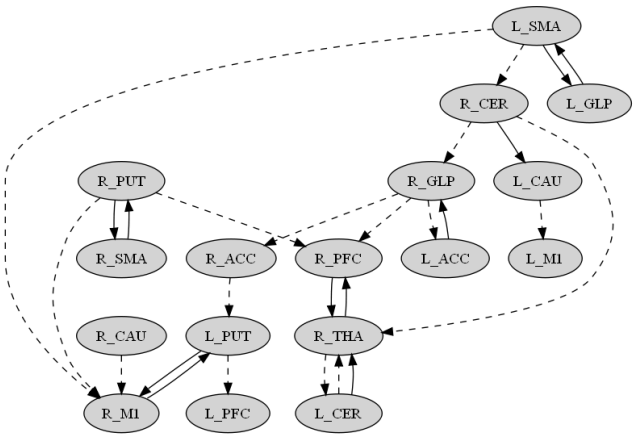

Fig. 3. The significant different connections between N and P_{pre} groups, derived from from the full SEM+MAR model. Solid lines are the SEM connection and dashed lines are the 1[th]-order mAR connections.

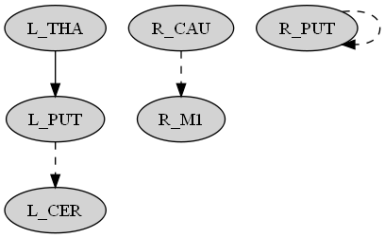

Fig. 4. The significant different connections between P_{pre} and P_{post} groups, learned from the proposed sparse model. Solid lines are the SEM connection and dashed lines are the 1[th]-order mAR connections.

connections derived from the traditional full model between N and P_{pre} groups, Fig.3.

Figure 2 demonstrates that the sparse model correctly identifies the importance of the prefrontal cortex (R PFC) in performing the motor task that may be affected in PD. The prefrontal cortex, especially the dorsolateral part, is responsible for motor planning, organization, and regulation, and interestingly has been considered a target for PD treatment by Transcranial Magnetic Stimulation [12]. The effects of medication on the sparse model are shown in Figure 4. These significant connections emphasize that connections between basal ganglia structures such as the thalamus, putamen, and caudate, normally affected by PD, are modulated by L-dopa medication.

V. CONCLUSION

The proposed sparse joint SEM and mAR model has been demonstrated to be more accurate for inferring connectivity between regions in simulations. When applied to real fMRI data, the proposed method demonstrated few connections in plausible regions. We suggest that the method is more appropriate for fMRI studies, when the ratio of the number of ROIs to the number of time points may be large.

ACKNOWLEDGMENT

This work was supported in part by the Canadian Natural Sciences and Engineering Research Council (NSERC) and Canadian Institutes of Health Research (CIHR).

REFERENCES

[1] A. McIntosh, C. Grady, L. Ungerleider, J. Haxby, and et al., "Network analysis of cortical visual pathways mapped with pet," *Journal of Neuroscience*, vol. 14, no. 2, pp. 655–666, 1994.
[2] W. P. Harrison, L. and K. Friston, "Multivariate autoregressive modeling of fmri time series," *Neuroimage*, vol. 19, no. 4, pp. 1477–91, 2003.
[3] M. Goncalves and D. Hall, "Connectivity analysis with structural equation modelling: an example of the effects of voxel selection," *Neuroimage*, vol. 20, no. 3, pp. 1455–67, 2003.
[4] J. Kim, W. Zhu, L. Chang, P. M. Bentler, and T. Ernst, "Unified structural equation modeling approach for the analysis of multisubject, multivariate functional mri data," *Human Brain Mapping*, vol. 28, pp. 85–93, 2007.
[5] S.-B. J. Valdes-Sosa, Pedro and et al., "Estimating brain functional connectivity with sparse multivariate autoregression," *Phil. Trans. R. Soc. B*, vol. 360, pp. 969–81, 2005.
[6] X. Chen, J. Z. Wang, and M. J. McKeown, "A fully bayesian approach on sparse linear regression," *IEEE Transaction on Signal Processing (submitted)*, 2008.
[7] R. Tibshirani, "Regression shrinkage and selection via the lasso," *J. Royal. Statist. Soc B.*, vol. 58, pp. 267–288, 1996.
[8] P. Green, "Reversible jump markov chain monte carlo computation and bayesian model determination," *Biometrika*, vol. 82, pp. 711–732, 1995.
[9] S. Richardon and G. Peter, "On bayesian analysis of mixtures with an unknown number of components," *J. Royal. Statist. Soc B.*, vol. 59, no. 4, pp. 731–792, 1997.
[10] B. Efron, T. Hastie, I. Johnstone, and R. Tibshirani, "Least angle regression," *Annals of Statistics*, vol. 32, no. 2, pp. 407–499, 2004.
[11] S. Palmer, L. Eigenraam, T. Hoque, R. McCaig, A. Troiano, and M. McKeown, "Levodopa-sensitive, dynamic changes in effective connectivity during simultaneous movements in parkinson's disease," *Neuroscience (in press)*, 2008.
[12] del Olmo M.F., O. Bello, and J. Cudeiro, "Transcranial magnetic stimulation over dorsolateral prefrontal cortex in parkinson's diseasen," *Clinical Neurophysiology*, vol. 118, no. 1, pp. 131–139, 2007.